第29卷 第4期
2005年4月

高 能 物 理 与 核 物 理
HIGH ENERGY PHYSICS AND NUCLEAR PHYSICS

Vol.29, No.4
Apr., 2005

Experimental Study of a Small-cell Drift Chamber Operated with Helium-Based Gases

LIU Jian-Bei[1,2;1)] CHEN Chang[1] CHEN Yuan-Bo[1] JIN Yan[1] LIU Rong-Guang[1]
MA Xiao-Yan[1] MA Yuan-Yuan[1] QIN Zhong-Hua[1,2] TANG Xiao[1] WANG Lan[1]
WU Ling-Hui[1,2] XU Mei-Hang[1] ZHU Min-Xuan[1] ZHU Qi-Ming[1]

1(Institute of High Energy Physics, CAS, Beijing 100049, China)
2(Graduate School of the Chinese Academy of Sciences, Beijing 100049, China)

Abstract The performance of a small-cell drift chamber operated with two helium-based gas mixtures, $He/C_3H_8(60/40)$ and $He/CH_4(60/40)$, was studied using cosmic rays, respectively. The gas mixture $Ar/CO_2/CH_4(89/10/1)$ was also tested for comparison. The spatial resolution and dE/dx resolution of the helium-based gases are better than those of $Ar/CO_2/CH_4(89/10/1)$. A good spatial resolution of 110μm and a dE/dx resolution of 6%—7% with 30—40 samples were obtained with $He/C_3H_8(60/40)$.

Key words drift chamber, small cell, helium-based gas mixture

1 Introduction

The BES Ⅲ[2)] experiment is designed to perform high-precision measurements and new physics search at the tau-charm factory BEPC Ⅱ[3)]. This places stringent demands on the performance of the drift chamber for BES Ⅲ. It must provide high efficiency, good momentum resolution and excellent adaptability for high count rate. In addition, the drift chamber is required to serve particle identification with ionization loss(dE/dx) measurements. The solution to meet the above requirements is a small-cell drift chamber made of low mass material[2)]. The small cell design has many advantages with good spatial resolution, good dE/dx resolution, long aging lifetime and fast response. The latter two are essential for the operation under the high luminosity condition of BEPC Ⅱ. The majority of charged particles produced in BEPC has the momentum lower than 1GeV/c. The predominant limitation on the momentum resolution is the error due to the multiple scattering in the drift chamber. It can be minimized by reducing the amount of material in the drift chamber. So the light gas is preferred. The helium-based gas is the good candidate for such kind of gas. In addition, the helium-based gas can reduce the background from large amount of synchrotron radiation produced in the collider with high luminosity for its small photo-electric cross section.

So far, many kinds of helium-based gases have been studied[1—5]. The small-cell drift chamber has also been successfully used in many large experiments of high energy physics[6—8].

In order to study the performance of the small-cell drift chamber filled with helium-based gas mixtures, we built a prototype drift chamber with the cell size similar to the design of the BES Ⅲ drift chamber and carried out some tests using cosmic rays. In this paper, we present the test results of the prototype drift chamber with two helium-based gas mixtures: $He/C_3H_8(60/40)$ and $He/CH_4(60/40)$, using cosmic rays. The gas mixture of $He/C_3H_8(60/40)$ is the perfect candidate for the BES Ⅲ drift chamber with its excellent properties of good spatial and dE/dx resolution and long radiation length

Received 2 September 2004

1) E-mail: liujb@mail.ihep.ac.cn

2) BES Ⅲ Preliminary Design Report. IHEP-BEPC Ⅱ-SB-13, 2004.

3) BEPC Ⅱ Preliminary Design Report. 2002.

(550m). The gas mixture of $He/CH_4(60/40)$ is also interesting for its low price, easy access and very long radiation length(800m). In addition, the properties of $Ar/CO_2/CH_4$ (89/10/1), which was used by the BES Ⅱ drift chamber, were measured for comparison.

2 Experimental setup

The test chamber consists of 14 sense wire layers with 5 cells per layer, as shown in Fig.1. The cells are all in standard square shape to simplify the drift distance-time calibration, with the size of 16.4mm × 16.4mm. Each cell has one sense wire surrounded by a square grid of 8 field wires which

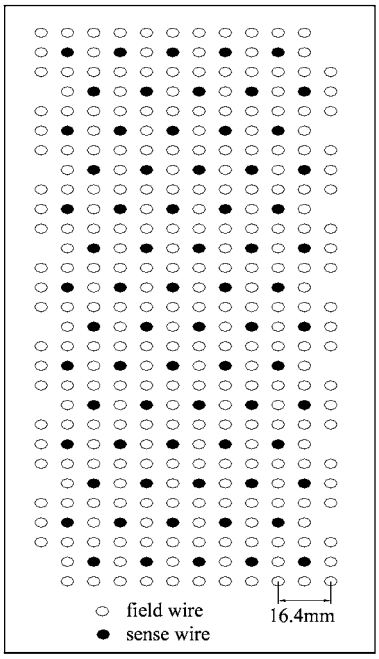

Fig. 1. The cell configuration of the test chamber.

are shared by adjacent cells. The sense wire is made of gold-plated tungsten(3% Re), 25μm in diameter, tensed with a weight of 20g. The field wire is made of gold-plated aluminum with a diameter of 110μm. A tension of 60g is applied to the field wires to match the gravitational sag of the sense wires. The wires are about 60cm long. All layers are axial with half cell staggering for left-right ambiguity resolution. The end-plates and the walls of the test chamber are all made of aluminum. A piece of 1cm long slit is machined in the middle of the upper wall to allow the use of ^{55}Fe X-ray to test the operation of the chamber. The high voltage is applied to the sense wires by a printed board at one end-plate, while the preamplifier boards are mounted on the other end-plate. The field wires are all connected to ground directly. The operating voltages for various gases are determined in such a way that the gas gains are similar.

The chamber was tested with various gases using cosmic rays. The test setup and electronics have been described in detail in Ref.[9].

The gas mixture He/C_3H_8 (60/40) was supplied by mass flowmeters. For He/CH_4 (60/40) and $Ar/CO_2/CH_4$ (89/10/1), pre-mixed gases were used.

3 Results and discussion

3.1 Drift distance-time relation

The data of cells used in analysis are required to have a drift time less than 500ns and a charge larger than the probable pedestal by 5 times' standard deviations. These cells are called hit cells. The probable pedestal and standard deviation are obtained by fitting the pedestal distribution to a Gaussian.

The electric field in the square small cell is not uniform because of the cell's geometric structure. As a result, the drift distance-time relation (x-t relation) for the cell is nonlinear. So an iterative algorithm is used to determine the x-t relation. With a rough x-t relation and after simple pattern recognition the track is fitted to the circles centered at the sense wires and with the radii corresponding to the measured drift distance of hit cells. Then the residuals for each drift time bin, defined as the signed difference between the drift distance calculated with drift time using x-t relation and the distance from the sense wire to the fitted track, are histogrammed. Each cell used for the calculation of residuals is excluded from the track fit to make the residual distribution bias free. The x-t relation is then corrected in each time bin by the average residual value. The new x-t relation is used in the next iteration. The x-t relation converges after a few iterations. In the iteration process, the adjustments of fine T0 and wire position are performed channel by channel, based on the residual distributions on the left and right side of sense wires to make the distributions center at about zero.

The x-t relations for various gas mixtures are all nonlinear as shown in Fig.2. $He/CH_4(60/40)$ has a smaller nonlinearity compared with $He/C_3H_8(60/40)$. This is consistent with the fact that $He/CH_4(60/40)$ has a lower electric field for the saturation of the electron drift velocity. The drift ve-

locities of helium-based gases are slower than $Ar/CO_2/CH_4$ (89/10/1) but still fast enough so that the maximum drift time for about 8mm distance at normal incident angle is less than 300ns. It is acceptable for BEPC Ⅱ.

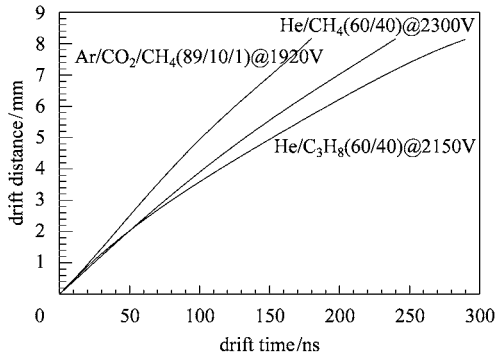

Fig. 2. *x-t* relations for various gases.

3.2 Spatial resolution

The spatial resolution is determined from the residual distribution. The width of the residual distribution has two contributions which add in quadrature: the intrinsic spatial resolution and the error of the track fit. So the residual has to be corrected to get the intrinsic spatial resolution without the track fit error. The time walk correction is also applied to improve the spatial resolution, based on the correlation of the timing and the pulse height.

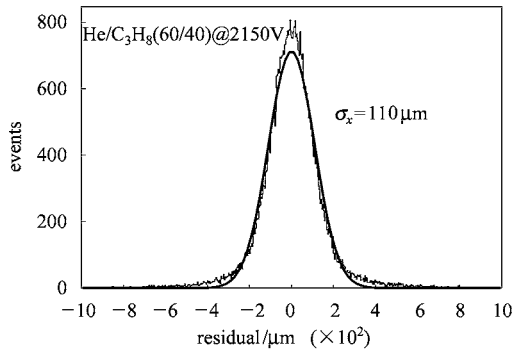

Fig. 3. The typical residual distribution.

The typical overall residual distribution after the above two corrections is shown in Fig. 3. The average spatial resolution is extracted by fitting the distribution to a Gaussian as shown in Fig. 3. The distribution has a pronounced non-Gaussian tail. It originates from the large spread of the drift time for the electrons ionized along the incident track to reach the sense wire, which is called non-isochronous behavior. This is the primary factor limiting the spatial resolution for the small cell.

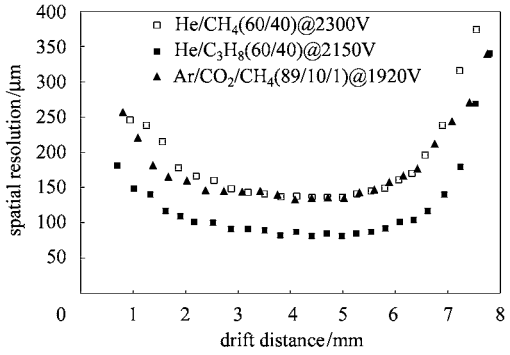

Fig. 4. The spatial resolution as a function of drift distance.

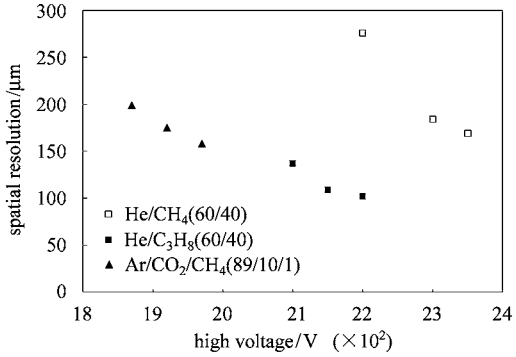

Fig. 5. The spatial resolutions of various gases as a function of the operating voltage.

The dependence of the spatial resolution on the drift distance is shown in Fig. 4. The spatial resolution deteriorates near the sense wire because of the statistic fluctuation of primary ionization and the sharp degradation near the cell edge is due to the distortion of the electric field. The spatial resolution for various gases is summarized in Fig. 5 as a function of the operating voltage. It is universal that the spatial resolution is improved significantly with the increase of the operating voltage when the high voltage is relatively low. He/C_3H_8 (60/40) achieves a spatial resolution of 110μm at 2150V. The spatial resolution of He/C_3H_8 (60/40) is much better than that of He/CH_4 (60/40). This is due to the fact that He/C_3H_8 (60/40) provides a much larger number of primary ions (30ions/cm) than that of He/CH_4 (60/40) (10ions/cm). Although $Ar/CO_2/CH_4$ (89/10/1) has large primary ions (30ions/cm), its spatial resolution is very bad compared

with $He/C_3H_8(60/40)$. The reason may be that the operating voltage is low and the fluctuation of the drift velocity in the cell is big. The incident azimuthal angle dependence of the spatial resolution was also studied. The result shows no significant deterioration up to 13°.

3.3 dE/dx resolution

For dE/dx measurement, the track was also required to pass through about 25cm of lead. This eliminated the tracks with low momenta which have a large range of dE/dx. Before calculating the dE/dx resolution, some corrections are applied on the pulse height. At first the path length correction is done using the reconstructed track. Then the gas gain variation due to the pressure or temperature change is corrected run by run. The relative gain difference between sense wires is also corrected channel by channel.

In order to obtain the dE/dx resolution with the samples similar to the expectation from the BESⅢ drift chamber (about 40), several events are combined for the measurement. The dE/dx resolution is measured using the truncation technique[10] to minimize the contribution of the well-known Landau tail[11] to dE/dx resolution. With the truncation technique, a Gaussian-like dE/dx spectrum is produced. The spectrum is then fitted to a Gaussian. The dE/dx resolution is defined as the ratio of the standard derivation of the Gaussian to the peak value.

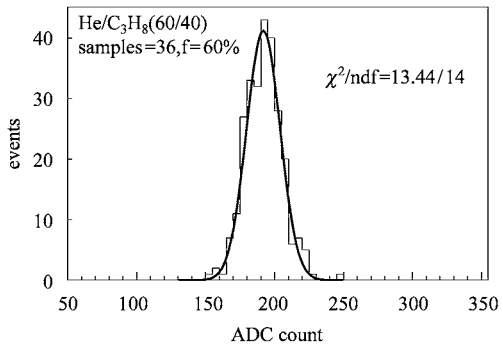

Fig. 6. The 60% truncated mean pulse height distribution.

Fig.6 shows the truncated mean pulse height distribution with 36 samples, 60% truncation fraction, for He/C_3H_8 (60/40) at 2150V. The distribution is quite Gaussian-like. The dE/dx resolution for various gases at various operating voltages is shown in Fig.7. $He/C_3H_8(60/40)$ has the best resolution for the presence of a large fraction of hydrocarbon. Despite the less primary ionization number, $He/CH_4(60/40)$ has a better dE/dx resolution than $Ar/CO_2/CH_4(89/10/1)$. This is because hydrocarbon gases have a very good dE/dx resolution[12]. The dependence of dE/dx resolution on the samples is also studied for $He/C_3H_8(60/40)$ at 2150V, as shown in Fig.8. A resolution of 6%—7% can be obtained with 30—40 samples.

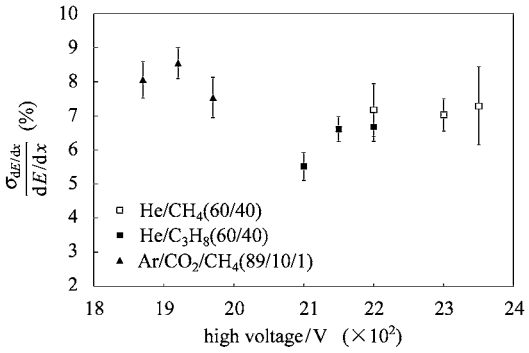

Fig. 7. The dE/dx resolution of various gases at several operating voltages.

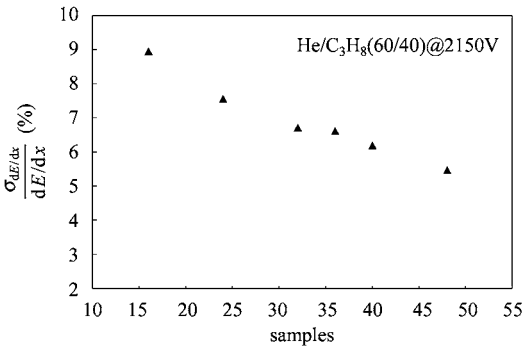

Fig. 8. The dE/dx resolution as a function of samples for $He/C_3H_8(60/40)$.

3.4 Cell efficiency

The cell efficiency is calculated to be the ratio of the tracks with hits in the cell within a 5-σ window to the total tracks passing through the cell, where σ is the average spatial resolution. Fig. 9 shows the cell efficiency as a function of the distance from the sense wire. The efficiency drops very quickly near the cell boundary. The drop arises from the small and slow signal when the track passes the cell boundary due to the very dispersed drift time for primary ionized electrons. This effect will be enhanced in the presence of the magnetic field. The efficiency for various gases at various operating voltages is shown in Fig. 10. The efficiency gets

higher with the increase of the operating voltage and then arrives at a plateau. The drift chamber should operate at the plateau of efficiency. $He/C_3H_8(60/40)$ achieves a better efficiency than the other gases with the similar gas gain.

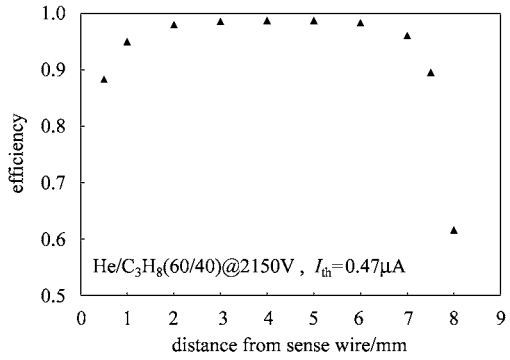

Fig. 9. The cell efficiency as a function of the distance from the sense wire.

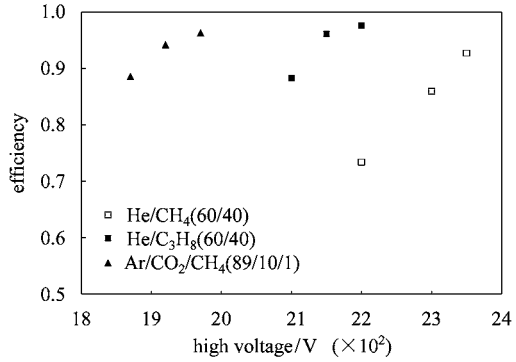

Fig. 10. The cell efficiency for various gases as a function of the operating voltage.

3.5 Cross-talk

The cross-talk between the neighboring cells is studied by comparing the ADC pedestal of one cell in the case of no hit in its neighboring cells with the case of having hits in the neighboring cells. A cross-talk of about -2.0% between the neighboring cells is found. It indicates that the major contribution to the cross-talk is the signal induced on the nearby sense wire by the motion of the positive ions produced in the avalanche. As the positive ions motion relative to the nearby sense wire is opposite to the sense wire in avalanche, the induced signal has an opposite sign. Anyway the cross-talk for small cell is small and does not produce spurious hits thanks to its opposite sign.

4 Conclusion

We have tested the performance of a small-cell drift chamber prototype with two helium-based gas mixtures: $He/C_3H_8(60/40)$ and $He/CH_4(60/40)$ as well as the mixture of $Ar/CO_2/CH_4$ (89/10/1), using cosmic rays. Our study shows that the helium-based gases provide better spatial and dE/dx resolutions than $Ar/CO_2/CH_4(89/10/1)$ and a good spatial resolution of 110μm and a dE/dx resolution of 6%—7% with 30—40 samples can be obtained using the small cell with the helium-based gas $He/C_3H_8(60/40)$. It indicates that the BESⅢ drift chamber can be considered to be a small-cell drift chamber operated with $He/C_3H_8(60/40)$ to satisfy its performance requirements.

References

1 Uno S et al. Nucl. Instrum. and Methods, 1993, **A330**:55
2 Playfer S M et al. Nucl. Instrum. and Methods, 1992, **A315**:494
3 Cindro V et al. Nucl. Instrum. and Methods, 1991, **A309**:411
4 Bernardini P et al. Nucl. Instrum. and Methods, 1995, **A355**:428
5 CHEN Chang et al. High Energy Physics and Nuclear Physics, 1998, **22**:787—793(in Chinese)
(陈昌等.高能物理与核物理,1998,**22**:787—793)
6 Hirano H et al. Nucl. Instrum. and Methods, 2000, **A455**:294
7 Peterson D et al. Nucl. Instrum. and Methods, 2002, **A478**:142
8 Sciolla G et al. Nucl. Instrum. and Methods, 1998, **A419**:310
9 CHEN Jun et al. Nuclear Electronics & Detection Technology, 2004, **23**:159(in Chinese)
(陈君等.核电子学与探测技术,2004,**23**:159)
10 Jeanne D et al. Nucl. Instrum. and Methods, 1973, **A111**:287
11 Landau L.J. Phys. (USSR), 1994, **8**:201
12 Lehraus I et al. Nucl. Instrum. and Methods, 1982, **A200**:199

一个使用氦基混合气的小单元漂移室的实验研究

刘建北[1,2;1)] 陈昌[1] 陈元柏[1] 金艳[1] 刘荣光[1] 马骁妍[1] 马媛媛[1]
秦中华[1,2] 唐晓[1] 王岚[1] 伍灵慧[1,2] 徐美杭[1] 朱旻萱[1] 朱启明[1]

1(中国科学院高能物理研究所 北京 100049)
2(中国科学院研究生院 北京 100049)

摘要 利用宇宙线分别研究了一个小单元漂移室在 $He/C_3H_8(60/40)$和 $He/CH_4(60/40)$两种氦基混合气下的性能.作为比较还测试了在 $Ar/CO_2/CH_4(89/10/1)$混合气下的性能.研究表明上述氦基混合气的空间分辨和 dE/dx 分辨好于 $Ar/CO_2/CH_4(89/10/1)$混合气.使用 $He/C_8H_8(60/40)$可以获得 110μm 的空间分辨,在 30—40 次取样下 dE/dx 分辨可以达到 6%—7%.

关键词 漂移室 小单元 氦基混合气

2004-09-02 收稿

1) E-mail:liujb@mail.ihep.ac.cn